Materials Letters 138 (2015) 184–187

Contents lists available at ScienceDirect

Materials Letters

journal homepage: www.elsevier.com/locate/matlet

Hierarchically textured surfaces of versatile alloys for superamphiphobicity

Haiping Yu [a], Xin Tian [a], Hao Luo [a], Xiaolei Ma [a,b,*]

[a] NanoBiophotonics Center, National Key Laboratory and Incubation Base of Photoelectric Technology and Functional Materials, School of Physics, Northwest University, Xi'an 710069, PR China
[b] Department of Physics, Emory University, Atlanta 30322, GA, USA

ARTICLE INFO

Article history:
Received 7 July 2014
Accepted 2 October 2014
Available online 14 October 2014

Keywords:
Wetting
Superamphiphobicity
Contact angle
Hierarchical structures

ABSTRACT

We herein report a facile approach to realize superamphiphobicity based on versatile engineering alloys. Conventionally, the methods employed to endow solid surfaces with super-nonwetting properties rely on complicated manufacturing processes of micro/nanoscale structures or delicate chemical modifications or their combinations, however, suffering from high costs and complexity. In this work, superamphiphobicity is successfully obtained through a facile two-step method. We employ the chemical corrosion process to create surface with microscale roughness followed by the deposition of candle soot film with nanoscale textures, obtaining the hierarchical structures resultantly which could satisfactorily account for the physical origin of the superamphiphobicity here: superhydrophobicity with a water contact angle (CA) of $\sim 160^\circ$, and near-superoleophobicity with a glycerol CA of $\geq 130^\circ$. Our method offers the industrial community a novel approach for manufacturing self-cleaning and antifouling smart materials.

1. Introduction

Super-nonwetting phenomena are drawing extensive concern recently [1]. One famous example in nature exhibiting super-nonwettability is the lotus leaf which shows super-water-repellency, demonstrating huge advantages in self-cleaning [2]. Besides, superoleophobicity which repels oily liquid has also attracted increasing attention due to the promising potential in antifouling [3]. Therefore, generating superamphiphobicity that contains both superhydrophobicity and superoleophobicity is increasingly demanded in industries for versatile practical applications [4].

It is well documented that wetting behavior of a solid surface is controlled by its chemical compositions and surface roughness [5,6]. Generally, the decrease of surface energy can enhance wettability; however, the maximum CA for a water droplet resting on a smooth surface with extremely low surface energy is $\sim 120^\circ$, leading to the necessity of modulating surface roughness combined with chemical modifications in order to obtain super-nonwettability. Motivated by this, Chen et al. [7] obtained a superhydrophobic TPU film with bead-on-string morphologies through electrospinning. Besides, it is rather difficult to repel organic liquids due to the van der Waals forces which enable the liquids to spread easily. Therefore, it is even harder to realize superamphiphobicity, for which two basic criteria should be satisfied. One is the construction of rough surfaces like reentrant or overhanging structures [8] which are effective to trap air/bubbles. The other is the modification of chemicals whose surface tensions are basically lower than a quarter of that of probing oils. Even more recently, Deng et al. [9] developed a robust, transparent, superamphiphobic surface via the combinations of fractal network deposition and fluorinated silane modification based on a glass slide, which, however, suffers from complexity and high cost.

In this work, we successfully realize superamphiphobicity via a facile two-step method based on versatile engineering alloys. Briefly, we perform the chemical corrosion to obtain microscale surface roughness followed by the deposition of candle soot with nanoscale surface roughness, obtaining the hierarchical structures that account for the superamphiphobicity in our experiments.

2. Experimental

Materials and solutions: Engineering Mg, Al, and Ti alloy slides with the dimension $\sim 2.0 \times 3.0\ cm^2$ are used as substrates. Different levels of the silicon carbide (SiC) and diamond paste are utilized to modify the substrates. Finally, three categories of the samples are prepared: (1) rough sample (polished with 80 grit

* Corresponding author at: Department of Physics, Emory University, Atlanta 30322, GA, USA. Tel.: +1 404 615 4868.
E-mail address: xiaolei.ma@emory.edu (X. Ma).

http://dx.doi.org/10.1016/j.matlet.2014.10.015
0167-577X/

sheet); (2) semi-polished sample (polished with 80, 320, 600 and 800 grit sheets in sequence); (3) finely polished sample (polished with 80, 320, 600, 800, 1200, 1500, 2000 grit sheets and 1.5 μm diamond paste in sequence). Hydrogen chloride (HCl), oxalic acid (HOOCCOOH), potassium permanganate (K_2MnO_4) solutions are purchased from Beijing Chemical Engineering Co., Ltd.

Fabrication of hierarchical structures and CA measurement: First, the as-prepared samples are corroded to obtain microscale textures. Second, candle soot film is deposited onto the corroded samples to obtain nanoscale textures. Briefly, for Mg samples, corroded with 30 mL, 1 M HCl solution mixed with 30 mL, 0.1 M HOOCCOOH solution for 5 min, then removed and cleaned with Di-water, afterwards soaked in 0.1 M K_2MnO_4 solution for 1 h to activate the corroded surfaces, finally dried with nitrogen and kept in dry environment. The corroded samples are then placed to contact the top of candle flame to automatically deposit flame soot onto the surfaces. The deposition lasts ~2 s for one spot, the same deposition procedure is repeated for other spots until the whole substrate is covered by a uniform soot film. The samples are then cooled down to room temperature (RT ~25 °C) to perform CA measurement. Similarly, for Al samples, corroded with mixed acidic solutions of 30 mL, 2 M HCl and 30 mL, 0.1 M HOOCCOOH for 5 min; for Ti samples, corroded with mixed acidic solutions of 30 mL, 3 M HCl and 30 mL, 0.1 M HOOCCOOH for 18 h. The candle soot deposition procedure for Al and Ti samples is similar to that of Mg samples.

In CA measurement (at RT), water and glycerol droplets are used. By using a microsyringe, the droplets (~10 μL) are gently deposited onto each substrate perpendicularly. The images of the droplets resting on the substrate are captured by a CCD system (F201-B+Nikkor 60 mm/2.8 lens) and analyzed by ImageJ to obtain CA (the reported CA is the mean value of five different measurements for each sample). A scanning electron microscope (SEM, JSM6390A, Japan) is employed to obtain the surface morphology.

3. Results and disscussion

Initial surface wettability: We investigate the effect of initial surface roughness on the wettability by employing water and glycerol whose surface tensions are 72.8 and 63.6 mN/m, respectively. The results are displayed in Fig. 1. (We here only show the results of Mg samples.)

It is can be concluded from Fig. 1 that the CAs decrease with the increase of surface roughness in the hydrophilic regime. This can be explained by Wenzel model [10] (Fig. 2b):

$$\cos\,\theta_W = r\,\cos\,\theta \tag{1}$$

where r is the roughness factor defined as the ratio of the actual solid–liquid contact area to the projected area on the horizontal surface, θ is the intrinsic CA of the flat surface given by Young model (Fig. 2a):

$$\cos\,\theta = \frac{\gamma_{sv}-\gamma_{sl}}{\gamma_{lv}} \tag{2}$$

where γ_{sv}, γ_{sl} and γ_{lv} are the interfacial surface tensions of solid/vapor, solid/liquid and liquid/vapor, respectively.

In Wenzel model, $r>1$, then surface roughness enhances hydrophilicity in the hydrophilic regime, which agrees with our results (Fig. 1). We demonstrate that the surface wettability is dependent on the surface roughness, additionally, when the surface tension of probing liquid is low enough, the influence of surface roughness becomes unpronounced as indicated by the CA of liquids with lower surface tensions as plotted in Fig. 3 (for Al and Ti samples, the tendency is similar to Mg samples).

Effect of hierarchical structures on wettability: It has been demonstrated that corrosion is a facile, effective method to create microscale textures by controlling the corrosion time properly [11]. Followed by this, here HCl is mixed with HOOCCOOH in the same volume to control the corrosion rate and strength in order to obtain microscale structures (the concentrations of acidic solutions here

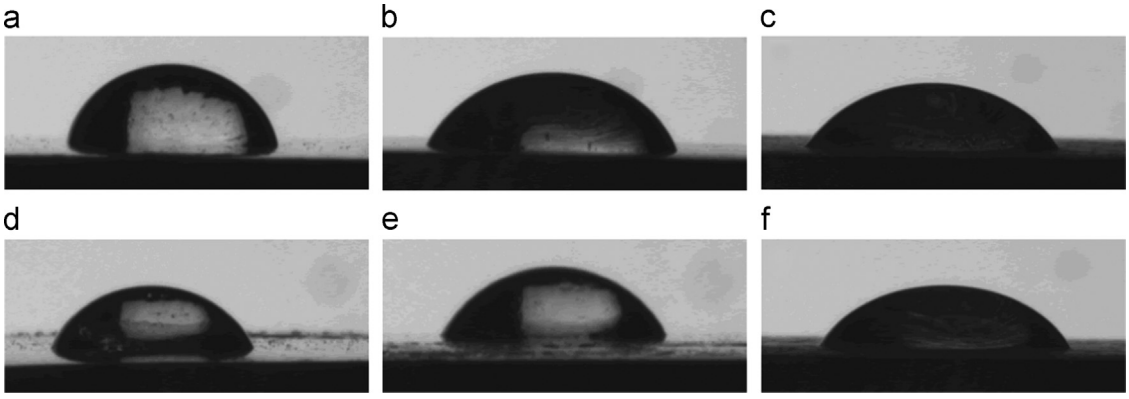

Fig. 1. Snapshots of water and glycerol droplets resting on (a), (d) finely polished; (b), (e) semi-polished; (c), (f) rough Mg samples before corrosion. The corresponding CAs are 70.5°, 59°; 57.8°, 55°; 45°, 43.6° for each column. The upper and lower panels are for water and glycerol droplets, respectively.

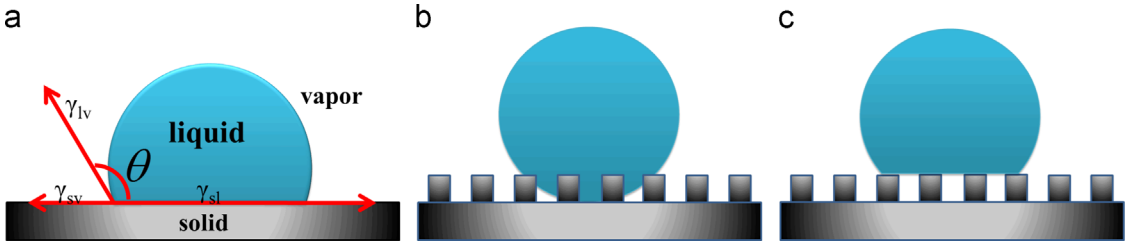

Fig. 2. Sketch of a droplet resting on a solid substrate. (a) A flat surface (Young model); (b) droplet penetrating into the grooves (Wenzel model); (c) droplet suspending on the peaks and air trapped in between grooves (Cassie–Baxter model).

are optimal after extensive trials). It is inevitable that there are kinds of defects inside the crystals, and the parts with higher energy will be first dissolved or corroded under acidic environment, thus creating microscale textures. As we stated in the previous study [11] that there are mainly three kinds of microscopic corrosion regimes, i.e., "pitting corrosion", "intergranular corrosion" and "general corrosion", which are dominant in different intervals throughout the corrosion process. The first two would tend to increase the surface roughness at the early stage, and then the "general corrosion" would be dominant in the later stage, which tends to decrease the surface roughness. Thus, by controlling the corrosion time, we can control the etching strength (etching depth) so as to obtain the desirable structures. Realistically the corrosion mechanism is rather complicated, and we here intentionally focus on the functionality of corrosion to generate microscale structures, and the deeper investigation on corrosion mechanism is thus not performed. After candle soot deposition, a fractal-like carbon nanosphere film is obtained on the surface, forming the hierarchical structures as illustrated by Fig. 4b and d (Mg and Ti samples are shown here). We once again utilize water and glycerol droplets to test the wettability of the obtained surfaces, and the results are shown in Fig. 4e.

It can be concluded from Fig. 4e that after corrosion and flame soot deposition, the three kinds of alloy samples exhibit superhydrophobicity, near-superoleophobicity. Additionally, the samples also exhibit drag-reducing capability (rolling off angles $\sim 10^\circ$ for water droplets). It is obvious that rough samples exhibit macroscale roughness with the textures of trenches or grooves as illustrated in Fig. 4a and c. After treating with our method, hierarchical structures are generated which contain microscale structures by corrosion and nanoscale structures created by deposition as illustrated by Fig. 4b and d. The huge wettability difference indicated by Fig. 1 and Fig. 4e demonstrates the effectiveness of our method to realize superamphiphobicity. Although the key factors for superamphiphobicity are still not clear, we would like to introduce the binary cooperative complementary concept to explain it which treats the superamphiphobic surfaces here as convex and concave binary cooperative complementary surfaces [12], where hierarchical structures lead to a sharp rise in surface roughness, and can stabilize the air trapped in concaves, thus forming a steady air film. Additionally, the nanoscale convex roughness (Fig. 4b and d) can provide a sufficient energy barrier against wetting [13], which makes superamphiphobicity possible. Also, the superhydrophobicity here can be further understood by Cassie–Baxter model [14] (Fig. 2c):

$$\cos\theta_{CB} = f_1 \cos\theta - f_2 \quad (3)$$

where f_1 and f_2 are area fractions of solid and air of the rough surface ($f_1+f_2=1$), θ_{CB} is the apparent CA of water droplet, and θ is the intrinsic CA of the flat surface. Apparently, θ_{CB} is a decreasing function of f_1 for a given θ. Therefore, to obtain a superhydrophobic surface, the contribution of the solid part should be small enough, which meets the effect of the hierarchical structures obtained in our work. Taking Mg samples for example, θ_{CB} is $\sim 163^\circ$ (Fig. 4e), θ on a flat graphite surface is 86° [15] for water droplets. After calculation, f_1 and f_2 are ~ 0.04 and 0.96; this means that solid and air occupy 4% and 96% of the contact area between the water droplets and the hierarchical structures, respectively, which agrees well with Cassie–Baxter model.

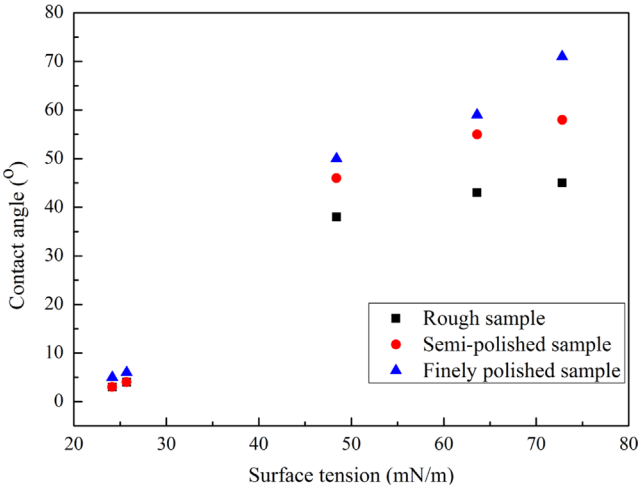

Fig. 3. Contact angles of droplets with different surface tensions on the surfaces of Mg samples with different surface roughnesses.

4. Conclusions

In summary, we successfully realize superamphiphobic surfaces via a two-step method: corroding the samples with acidic solutions followed by the flame soot deposition by burning candles, which endows the samples with hierarchical structures that account for the superamphiphobicity here: superhydrophobicity with a water CA of $\sim 160^\circ$ and near-superoleophobicity with a glycerol CA of $\geq 130^\circ$. What is more, the superamphiphobic surfaces are easy to be recovered if partly damaged mechanically. Our protocol is supposed to offer industries a novel approach

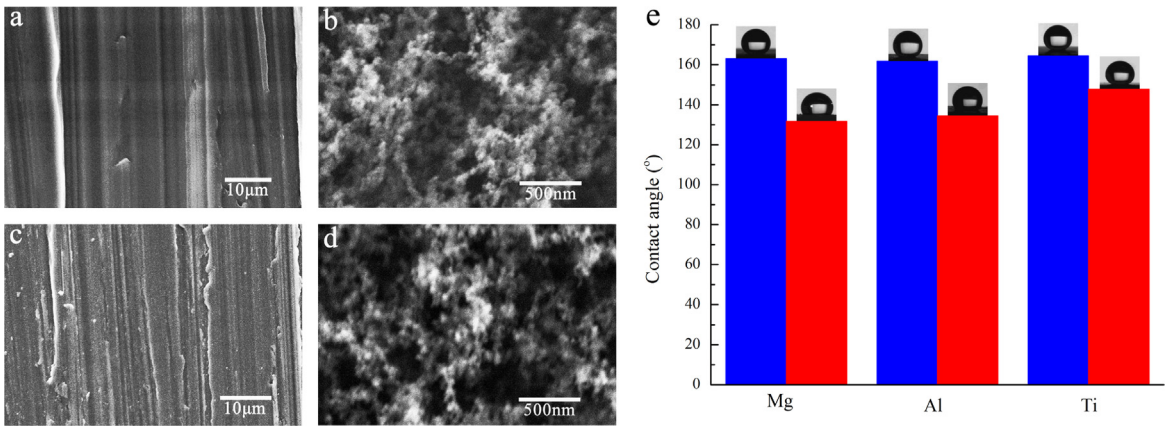

Fig. 4. SEM images and wettability of the samples. (a), (b) Mg samples, and (c), (d) Ti samples. (a), (c) Initially rough samples; (b) and (d) the rough samples after corrosion and candle soot deposition. (e) The wettability of the three kinds of initially rough alloy samples after corrosion and candle soot deposition tested by water (blue column) and glycerol (red column) droplets. The corresponding CAs for Mg, Al and Ti samples are 163.1°, 131.7°; 161.8°, 134.4°; 164.5°, 147.8°, respectively. (For interpretation of the references to color in this figure legend, the reader is referred to the web version of this article.)

for the mass-production of antifouling and self-cleaning smart materials.

Acknowledgments

The authors acknowledge the support by NSFC (No. 11104218), the Natural Science Basic Research Plan in Shaanxi Province of China (Program no. 2010JZ001), and the Scientific Research Foundation for Returned Overseas Chinese Scholars (Shaanxi Administration of Foreign Expert Affairs, 2011).

References

[1] Xia F, Jiang L. Adv Mater 2008;20:2842–58.
[2] Zorba V, Stratakis E, Barberoglou M, Spanakis E, Tzanetakis P, Anastasiadis SH, et al. Adv Mater 2008;20:4049–54.
[3] Kota AK, Li Y, Mabry JM, Tuteja A. Adv Mater 2012;24:5838–43.
[4] Liu K, Tian Y, Jiang L. Prog Mater Sci 2013;58:503–64.
[5] Ma J, Jing G, Chen S, Yu D. J Phys Chem C 2009;113:16169–73.
[6] Ma J, Jing G, Yu D. Soft Matter 2010;6:1527–32.
[7] Wang L, Yang S, Wang J, Wang C, Chen L. Mater Lett 2011;65:869–72.
[8] Choi HJ, Choo S, Shin JH, Kim KI, Lee H. J Phys Chem C 2013;117:24354–9.
[9] Deng X, Mammen L, Butt HJ, Vollmer D. Science 2012;335:67–70.
[10] Wenzel RN. J Phys Chem 1949;53:1466–7.
[11] Ma X, Luo H, Ma J, Wang P, Xu X, Jing G. Appl Phys A 2013;113:693–702.
[12] Jiang L, Wang R, Yang B, Li T, Tryk D, Fujishima A, et al. Pure Appl Chem 2000;72:73–81.
[13] Nosonovsky M. Langmuir 2007;23:3157–61.
[14] Cassie A, Baxter S. Trans Faraday Soc 1944;40:546–51.
[15] Liu H, Zhai J, Jiang L. Soft Matter 2006;2:811–21.